

Residual stresses at the surface of automotive suspension springs

M. T. TODINOV*

School of Metallurgy and Materials, The University of Birmingham, Edgbaston, Birmingham, B15 2TT, UK

E-mail: todinomt.st.met.bham@is-fsg.bham.ac.uk

This study concentrates on the origins of unfavourable stresses at the surface of silicon-manganese automotive suspension springs. The residual stresses have been investigated at the various stages of the spring manufacturing—quenching, tempering and shot peening. Residual stresses from quenching depend in a complex fashion on the microstructural state of the surface and on the variation of the thermal gradient into the quenched spring wire. Contrary to expectations, oil-quenching of decarburised spring wire results in tensile residual stresses at the surface, while water quenching results in compressive residual stresses. The residual stresses do not disappear after tempering. Moreover the shot peening after quenching and tempering, if not conducted properly, may result in small compressive or even tensile residual stresses at the surface, which severely diminishes the fatigue resistance of the suspension springs. © 2000 Kluwer Academic Publishers

1. Introduction

Typically, automotive suspension springs are manufactured by hot winding. The cut-to-length cold-drawn spring rods are austenitised, wound into springs, quenched and tempered. This is followed by warm presetting, shot peening, cold presetting and painting (Heitmann *et al.* [1]).

Although residual stresses exert strong influence on the fatigue properties of the suspension springs, the available published data are scarce. Conventional processing often results in undesirable residual stresses at the spring surface. Semenov and Serebrin [2] measured tensile residual stresses at the surface of a decarburised spring steel (60Si2). For a decarburised layer of 50 μm , the residual stress was 260 MPa at a depth of 125 μm . The decarburisation depth correlated with the depth where the residual stress changed its sign but had no influence on the maximum tensile residual stress. Furthermore, in test-pieces heat treated in evacuated ampoules to prevent surface decarburisation, the magnitude of the tensile residual stress was low. According to Semenov and Serebrin [2], the reason for the tensile residual stresses at the surface is the loss of carbon which increases the coefficient of thermal expansion. During quenching, this causes more vigorous contraction of the surface layers in comparison with the inner layers. The second reason was found in the volumetric effect due to the different microstructure of the surface and the core.

It is clear that this reasoning should also apply to water quenching, in which case tensile residual stresses at

the surface should be expected. Contrary to these expectations, the experiments in this study demonstrated that the residual stress at the surface of decarburised spring wire quenched in still water, is compressive.

Shot peening [3, 4] has been used as an important element of the spring manufacturing technology in order to improve fatigue resistance. Compressive residual stresses from shot peening increase fatigue life by delaying the initiation and inhibiting the propagation of fatigue cracks. The magnitude of the service tensile stresses is also reduced, which results in a smaller range of the net-tensile stress during fatigue tests. Shot peened helical springs can be used at 65–70% higher stress levels than unpeened springs. Shot peened leaf springs showed no failures at over 1000 000 cycles as compared with unpeened springs whose fatigue life was about 100 000 cycles [5].

Tensile residual stresses at the surface increase the effective net stress range and the mean stress during fatigue loading, which entails shorter fatigue crack initiation life and larger fatigue crack propagation rate. Unlike compressive residual stresses, the tensile residual stresses increase the negative effect from the damaged by shot-peening surface. Tensile residual stresses from quenching superpose with the compressive residual stresses from shot peening and form the net residual stresses. If the intensity of shot peening is small, the net residual stresses at the surface may even be dominated by a tensile component. Experimental measurements [6] identified zones of small compressive residual stress or even tensile residual stresses, beneath spring surface

* Formerly, with the Department of Materials Science and Engineering Technical University of Sofia, Bulgaria.

covered by shot-peening craters. These findings indicate that at some regions over the spring turns the shot peening intensity was not sufficient to create large and uniform compressive residual stress.

The outlined problems determined the aim of this study—analysis of the origins of unfavourable residual stresses at the surface of automotive suspension springs. Accordingly, the residual stresses were investigated at the key stages of the spring manufacturing—quenching, tempering and shot peening.

2. Residual stresses after quenching of silicon-manganese spring wire

All residual stress measurements on quenched and tempered spring wire were performed using an x-ray stress diffractometer [7]. The standard $\sin^2\psi$ method (Cullity, [8]; SAE [9]) employed was based on four inclined measurements at 0° , 15° , 30° and 45° . In order to minimise the instrumental error, only measurements of the axial residual stress (along the spring wire axis) were taken. The stress distribution with depth was produced by x-ray measurements followed by dissolving the surface layers. To ensure approximately equidistant sampling and little alteration of the measured residual stress, the surface layer was removed chemically, by a solution of nitric acid, applied gradually on top of the spring wire (Fig. 1a). The thickness of the removed layer was measured by a micrometer (Fig. 1b), at a constant location of the irradiated spot on the spring wire surface. Successively measured stresses at the surface were corrected by a small amount because of the stress relaxation created by the removed material (SAE, [9]).

Residual stress measurements in as-quenched silicon-manganese (0.6C-Si2-Mn1 spring steel) springs were performed. The specimens were taken from differ-

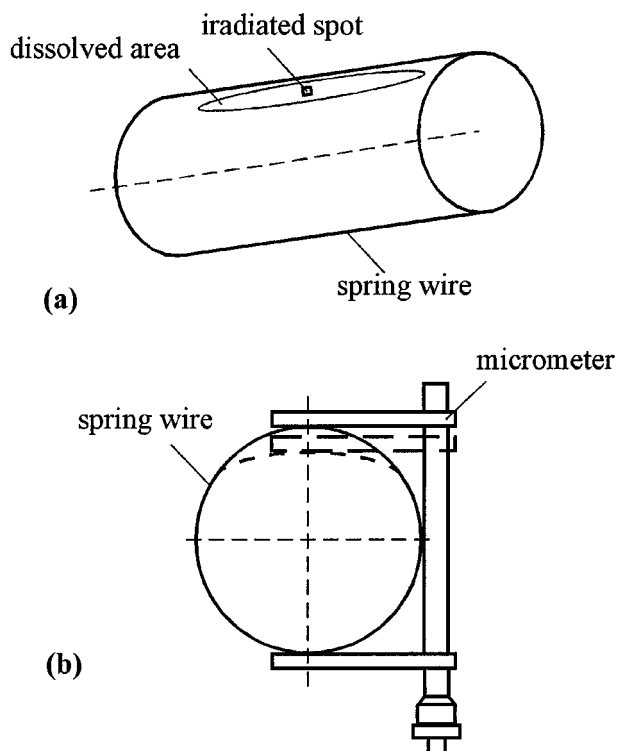


Figure 1 Measurement of the distribution of the axial residual stress with depth, after chemical dissolution of the surface layers.

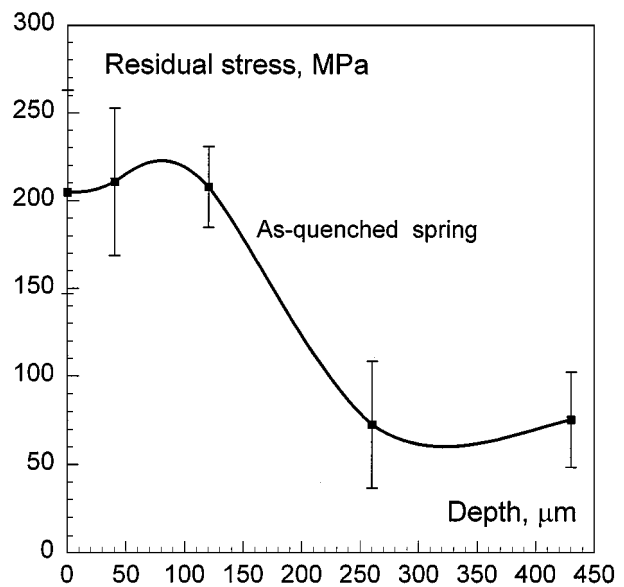


Figure 2 Residual stress distribution near the surface of an as-quenched silicon-manganese suspension spring.

ent turns of quenched in oil springs. All springs investigated exhibited tensile residual stress at the surface (Fig. 2), with an average value of +140 MPa. Variations of the tensile stress reaching +210 MPa were also indicated.

Residual stress measurements were also performed on 150 mm long specimens, taken from cold drawn cylindrical bars of diameter ~ 12 mm (0.6C-Si2-Mn1 spring steel). In order to eliminate the decarburisation during austenitisation, half of the specimens had been machined and sealed in quartz tubes filled with argon. (A completely decarburised surface layer of thickness 30–50 μm was measured in the decarburised specimens.)

Four types of quenching with no agitation were carried out, after austenitisation at 880°C for 20 min: (i) oil-quenching of non-decarburised specimens (NO); (ii) water-quenching of non-decarburised specimens (NW); (iii) oil quenching of decarburised specimens (DO) and (iv) water-quenching of decarburised specimens (DW).

Quench oil and tap water with temperature 20°C were used as cooling media, whose quantity was sufficient to prevent a substantial rise of temperature (which may otherwise alter the cooling properties). Quenching was carried out with no agitation. The cooling curves at the axis of the quenched spring wire are shown in Fig. 3. They were recorded by NiCr-Ni thermocouples of diameter 0.3 mm, embedded axially till the mid length of specimens cut from silicon-manganese spring wire. The specimens had a large length to diameter ratio (length 150 mm, diameter 12 mm) in order to approximate a one-dimensional heat transfer for the middle part where the hot junction of the thermocouple was located [6].

The non-decarburised oil-quenched specimens (NO) exhibited average residual stress at the surface close to zero (4.4 MPa, Table I). The non-decarburised water quenched specimens (NW) for nearly all of which the vapour blanket was unstable, exhibited compressive residual stress at the surface, of average magnitude -190 MPa (Table II). In few cases, however, where the

TABLE I Axial residual stress after oil-quenching measured at several locations at the surface of 14 non-decarburised specimens cut from silicon-manganese spring wire

-62.7 ± 22.5	-34.3 ± 23.5	-29.4 ± 19.6	-23.5 ± 53.9	-11.8 ± 27.4	-7.8 ± 11.8	-5.8 ± 43.1
0.0 ± 35.2	11.8 ± 7.8	23.5 ± 35.2	34.3 ± 8.8	46.0 ± 14.7	52.9 ± 21.6	68.6 ± 10.8

TABLE II Axial residual stress after water quenching characterised by an unstable vapour-blanket stage. The residual stresses were measured at several locations at the surface of 10 non-decarburised specimens cut from silicon-manganese spring wire

-250.8 ± 45.0 ;	-245.0 ± 49.0 ;	-233.2 ± 23.5 ;	-231.2 ± 69.6 ;	-227.4 ± 43.1 ;
-213.6 ± 13.7 ;	-160.7 ± 29.4 ;	-119.6 ± 49.0 ;	-119.2 ± 44.0 ;	-99.0 ± 57.8

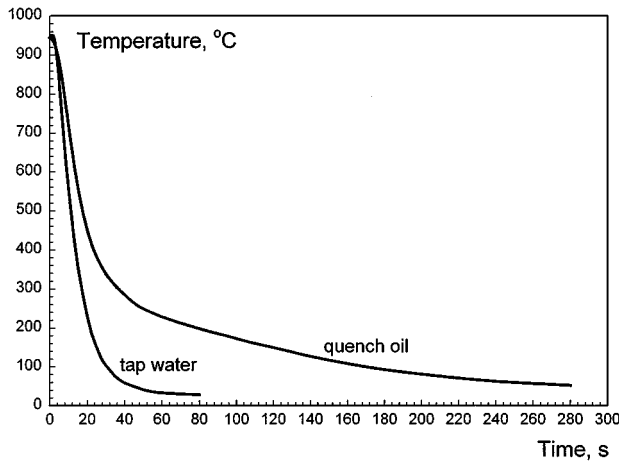


Figure 3 Cooling curves during quenching in oil and tap water, recorded by NiCr-Ni thermocouples of diameter 0.3 mm. The thermocouples were embedded axially, till the mid length of 150 mm long specimens cut from spring rods with diameter 12 mm.

vapour-blanket during quenching was relatively stable, some of the NW-specimens revealed at the surface residual stress varying around zero (0 ± 30 MPa) or tensile (40–100 MPa). Owing to fluctuations of the coefficient of heat transfer over the specimen-quenchant interface, in some cases the residual stress varied between tensile and compressive even on the same specimen.

Tensile residual stress measured after oil quenching of decarburised spring wire agreed with the experimental observations reported in Ref. [2]. Unlike the specimens from group NO, the decarburised specimens exhibited tensile residual stress at the surface (Fig. 4), after oil-quenching (specimens from group DO).

Similarly to the specimens from group NW, more than 80% of the decarburised water-quenched specimens (DW), showed compressive residual stress at the surface (Fig. 5).

3. Residual stresses after tempering of silicon-manganese spring wire

The spring wire was austenitised at 900 °C for 15 min, oil-quenched and tempered for different times in the temperature interval 400 °C–500 °C. After tempering, the tensile residual stress at the surface of oil-quenched decarburised springs, did not disappear. Tempering only diminished the magnitude of the tensile residual stress, causing stress relaxation proportional to tempering temperature and time. Fig. 6 shows the axial residual stress distributions measured near the surface

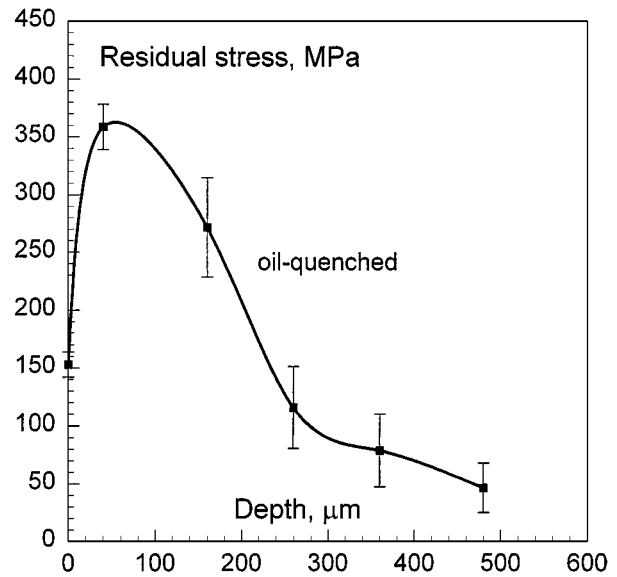


Figure 4 Residual stress distribution near the surface of oil-quenched decarburised silicon-manganese spring wire.

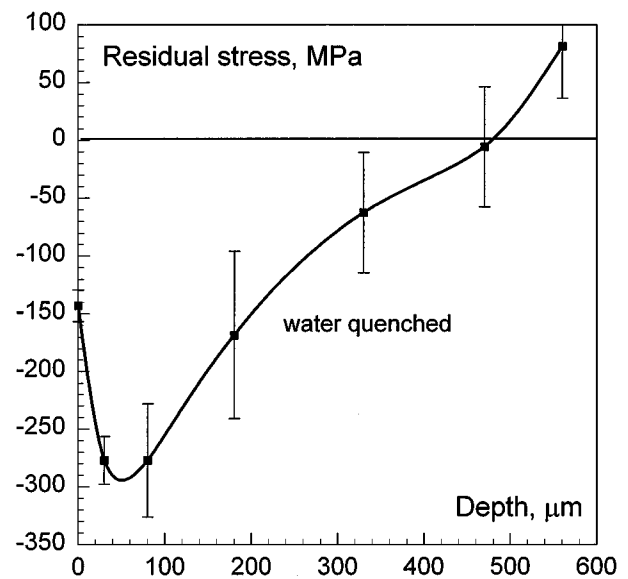


Figure 5 Residual stress distributions near the surface of decarburised silicon-manganese spring wire quenched in tap water.

of oil-quenched and tempered at 500 °C decarburised spring wire. During tempering, a considerable decrease of the residual stress magnitude from as-quenched state was registered within the first 14 minutes.

Fig. 7 shows tensile residual stress distributions measured in decarburised silicon-manganese spring wire, oil-quenched and tempered for one hour at 400 °C and

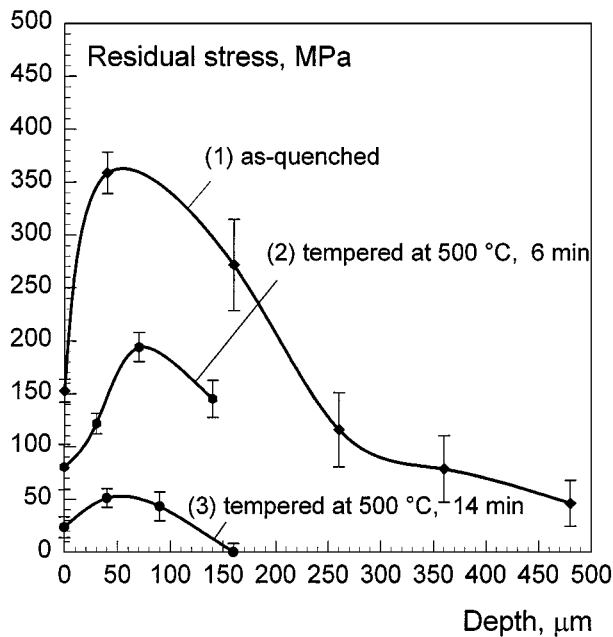


Figure 6 Residual stress distributions near the surface of decarburised silicon-manganese spring wire, quenched in oil and tempered at 500 °C, for 6 and 14 minutes.

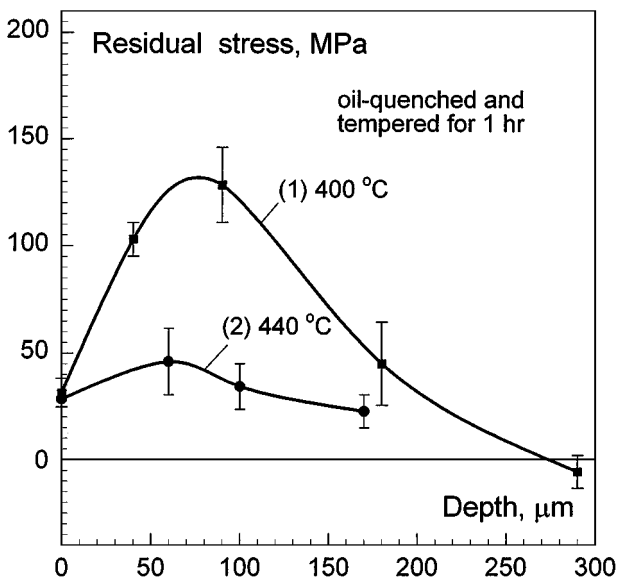


Figure 7 Residual stresses near the surface of decarburised silicon-manganese spring wire, quenched in oil and tempered at (1) 400 °C and (2) 440 °C for one hour.

440 °C. Tempering for 1 h at 400 °C resulted in a larger residual stress peak (~130 MPa) than tempering for 14 min at 500 °C (a residual stress peak of ~50 MPa).

The results in Figs 6 and 7 suggest that tempering temperature has a substantial influence on the level of the retained residual stress after tempering.

Stress relaxation of the compressive residual stress near the surface was also registered after water quenching and tempering. A typical residual stress distribution of quenched in still water and tempered for one hour at 400 °C decarburised spring wire is shown in Fig. 8.

Additional experiments were performed, in order to investigate the influence of the tempering regime on the magnitude of the tensile residual stress. Two different tempering regimes were selected, resulting in

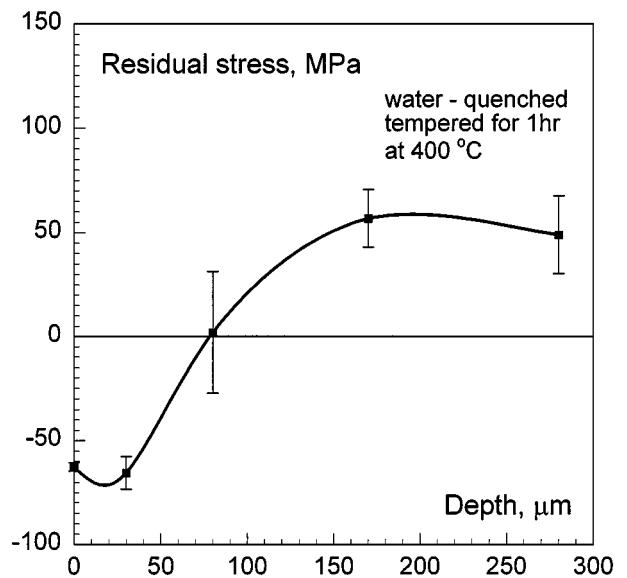


Figure 8 Residual stresses near the surface of decarburised silicon-manganese spring wire, quenched in water and tempered at 400 °C for one hour.

approximately the same hardness level of ~52 HRC. The first tempering regime consisted of tempering at 500 °C for 14 min; the second consisted of tempering at 440 °C for 60 min. Both tempering regimes resulted in residual stress distributions characterised by a tensile residual stress peak of approximately ~50 MPa (Fig. 6, curve 3 and Fig. 7, curve 2). The two tempering regimes, yielded the same average Vickers microhardness of 540 kg mm⁻² (~52 HRC) with a small variation over the cross section within 17 kg mm⁻². The tempering regimes did not result in large difference of the magnitude of the residual stress. This result implies a correlation between the residual stress magnitude and the hardness level, which is also supported by the residual stress distribution (1) from Fig. 7. Despite the relatively long tempering time (1 h) at temperature 400 °C, the tensile residual stress retained a relatively large magnitude, because the hardness level was relatively high (Vickers microhardness ≈600 kg mm⁻²).

4. Residual stress distributions after shot peening

The variation of shot peening intensity over the spring wire circumference was measured using the x-ray method described in Section 2. Again, in order to minimise the instrumental errors, all measurements were carried out, along the axis of the spring wire. During shot peening, the orientation of the spring turns regarding the trajectory of the peening shot is shown in Fig. 9. In the figure, 'λ' denotes the shot impact angle which the normal n^0 to the spring surface subtends with the incident trajectory of the peening shot; φ denotes the circumference angle; φ = 0° corresponds to the outside (o) and φ = 180°—to the inside (i) zone of the spring turn, while φ = ±90° correspond to the top (t) and bottom (b) zone of the spring turn, respectively.

The surface of all spring turns investigated was characterised by a 100% coverage from shot-peening.

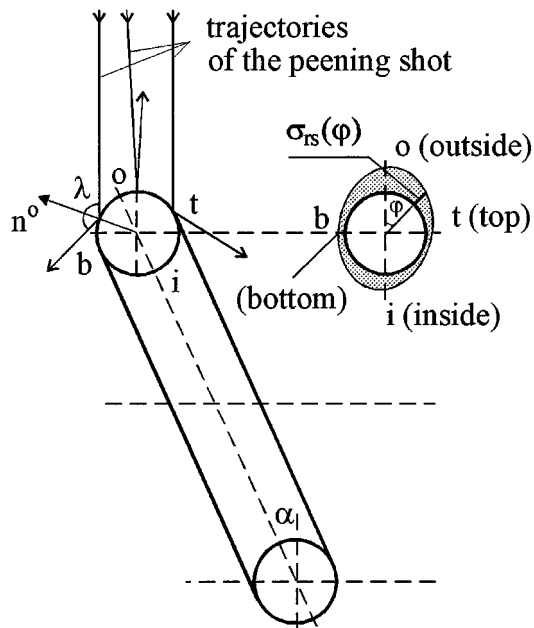


Figure 9 Orientation of the shot-peened spring turns regarding the trajectory of the peening shot.

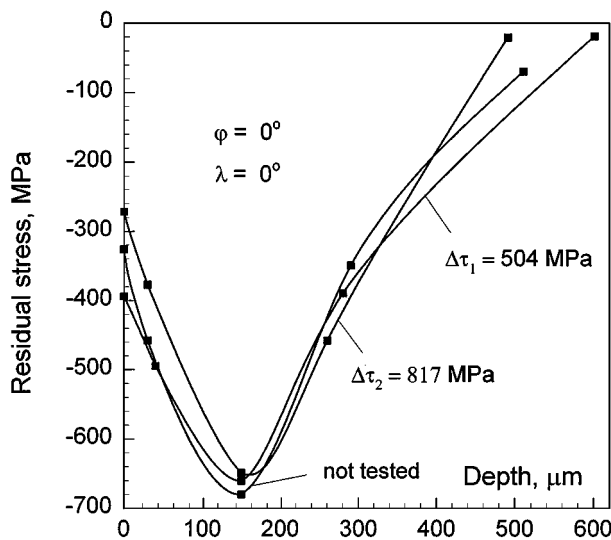


Figure 10 Residual stress distributions at the outermost part of the helix of silicon-manganese springs, before and after fatigue testing at shear stress ranges $\Delta\tau_1 = 504$ MPa and $\Delta\tau_2 = 817$ MPa.

Typical residual stress distributions after shot peening are characterised by a peak of the compressive residual stress, at some distance beneath the surface. On the outer surface of the helix (the best peened part) corresponding to a circumference angle $\varphi = 0^\circ$ and shot impact angle $\lambda = 0^\circ$, the maximum compressive stress was often in the interval $(-600, -700$ MPa), (Fig. 10).

The influence of cyclic loading on the magnitude of the residual stresses from shot-peening is of primary importance regarding the fatigue resistance of suspension springs. It was studied by measuring the residual stresses of three groups of springs, manufactured under the same conditions. One of the groups was not tested; the other two groups were fatigue tested at a maximum shear stress $\tau_{\max} = 1200$ MPa and shear stress ranges $\Delta\tau_1 = 504$ MPa (565000 cycles) and $\Delta\tau_2 = 817$ MPa (115000 cycles), respectively. In order to eliminate the

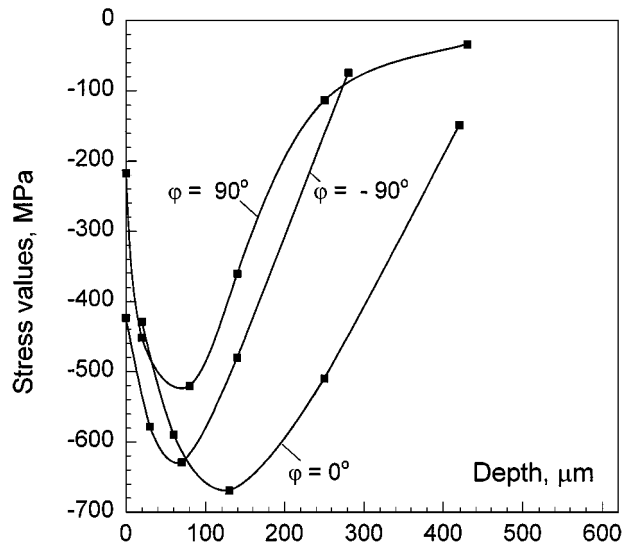


Figure 11 Residual stress distributions on the top ($\varphi = 90^\circ$), bottom ($\varphi = -90^\circ$) and outermost part of the helix ($\varphi = 0^\circ$) for a relatively uniformly shot-peened silicon-manganese spring (not tested).

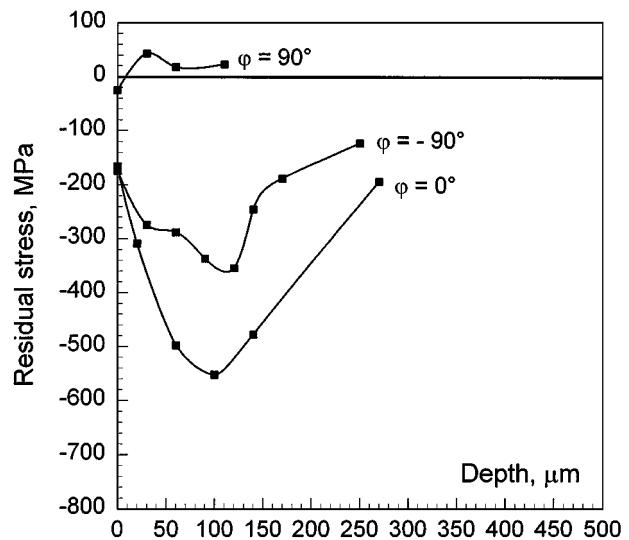


Figure 12 Residual stress variation over a turn of a non-uniformly shot-peened silicon-manganese spring.

influence of the variation of the residual stress over the spring wire circumference, only residual stress distributions corresponding to a shot impact angle $\lambda = 0^\circ$ (circumference angle $\varphi = 0^\circ$) were compared. A typical result is shown in Fig. 10. It indicates that silicon-manganese spring steels possess a high cyclic stability of the residual stress, which agrees with the experimental observations by Shiwaku *et al.* [10].

Residual stress distributions over the circumference of a relatively uniformly shot peened spring are shown in Fig. 11. The residual stresses were measured at the outer ($\varphi = 0^\circ$), at the top ($\varphi = +90^\circ$) and bottom ($\varphi = -90^\circ$) part of a spring turn.

In Fig. 12, residual stress distributions are given, measured at locations $\varphi = 0^\circ$ (the outermost region of the spring turn) and $\varphi = \pm 90^\circ$ (the top and bottom regions of the turns, see Fig. 9). Although the springs were fully covered by shot peening craters, few of them showed uniform compressive residual stress over the turns. The residual stress distributions were usually

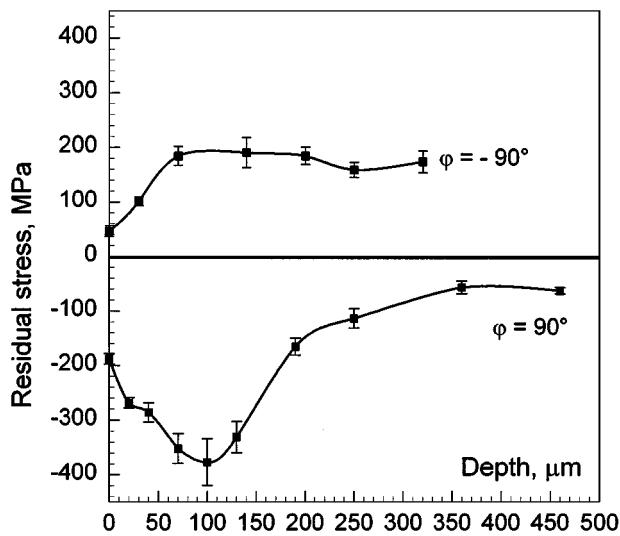


Figure 13 Tensile and compressive residual stresses on the opposite top and bottom regions of the same turn cut from a non-uniformly shot peened silicon-manganese suspension spring, tempered to a hardness level of 54 HRC.

compressive, but with large variation in the magnitudes which indicates uneven shot peening (Fig. 12). On some of the springs (Fig. 13) tensile residual stresses of relatively large magnitude were measured near the surface, although the entire circumference of their turns had been shot peened. In a number of instances, compressive and tensile residual stresses were measured on the same spring turn (Fig. 13). Tensile residual stresses at the surface were more frequently detected on springs tempered at a higher hardness level.

In some cases, the magnitude of the tensile residual stresses from tempering was relatively small and turned into compressive by the shot peening (Fig. 12, curve $\varphi = 90^\circ$). In other cases, the compressive residual stress from shot peening only decreased the magnitude of the tensile residual stress at the surface without being able to change its sign (Fig. 14a, $\varphi = 90^\circ$). In some cases where the tensile residual stress at the surface had been turned into compressive by shot peening, the resultant compressive residual stress had a relatively small magnitude (Fig. 14b, $\varphi = -90^\circ$).

5. Discussion

Residual stresses at the surface of automotive suspension springs depend on the microstructural state of the surface and the variation of the thermal gradient into the quenched wire. Oil quenching of non-decarburised spring wire resulted in residual stress at the surface close to zero, while for decarburised wire oil quenching resulted in substantial tensile residual stress. Contrary to expectations, water quenching without agitation resulted in compressive residual stresses for both type of specimens. The residual stress patterns from oil- and water-quenching of decarburised and non-decarburised specimens can be rationalised by the continuum model from Ref. [11]. According to the model, if during quenching of a cylindrical steel specimen, the net plastic strain generated during thermal contraction is smaller than that generated during transformation ex-

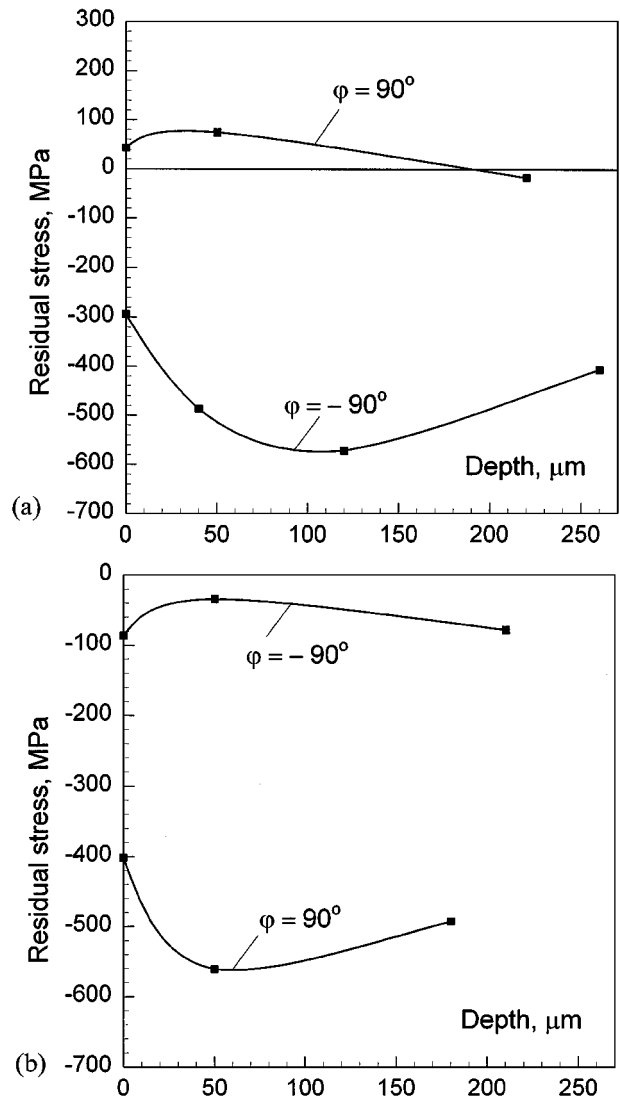


Figure 14 Residual stress distributions at the top and bottom regions of non-uniformly shot peened silicon-manganese suspension springs.

pansion, the residual stress at the surface is tensile. If the reverse is true, the residual stress is compressive.

Although quench oil produces small thermal gradients in the martensitic temperature interval, at high temperatures during the intensive thermal contraction it does not generate sufficient amount of plastic strain to compensate the tensile residual stresses due to decarburisation [11]. The tensile residual stress at the surface is due to the combined influence of the increased martensite start temperature of the decarburised surface and the larger coefficient of thermal contraction of the decarburised zones compared to the non-decarburised zones. Oil quenching of non-decarburised spring wire of diameter 12 mm, did not produce large residual stresses. Following the earlier discussion, this is due to the small thermal gradients produced by oil-quenching, which were unable to promote significant plastic flow during thermal contraction and transformation expansion. The result is no residual stresses or residual stresses of relatively small magnitude. The relatively large range of the residual stresses measured on the specimens is due to large variations in the intensity of quenching at high temperatures. This is also the reason for measuring residual stresses of opposite

sign on the same specimen. In places where the intensity of quenching had been large enough to produce some plastic strain, the residual stress was compressive of small magnitude. Conversely, in places where the amount of plastic strain had been very small or missing, the residual stress was zero or tensile of small magnitude.

By contrast, the compressive residual stresses at the surface after water quenching, are due to the large thermal gradients at high temperatures which resulted in large amount of plastic strain during thermal contraction. By the time of entering the transformation region, because of the relatively small diameter of the spring wire, the thermal gradient decreased significantly and the amount of net plastic strain generated by transformation expansion was not sufficient to dominate the net plastic strain from thermal contraction. As a result, the residual stress at the surface was compressive. After water quenching of decarburised specimens, the residual stress at the surface is compressive because the effect of the plastic strain created in the transformation region and the effect from the larger coefficient of thermal contraction of the decarburised surface (both promoting tensile residual stress at the surface) are outweighed by the large amount of plastic strain created from thermal contraction which entails compressive residual stress at the surface. At high temperatures, water-quenching creates much larger thermal gradients compared to oil-quenching. According to the continuum model proposed in earlier work [11] this leads to a compressive residual stress at the surface.

Apparently, the tensile residual stress at the surface detected in cases where the vapour blanket during water quenching was relatively stable, is caused by the decreased thermal gradient at high temperatures. At the same time, the thermal gradient in the transformation region remained practically unchanged. As a result, the amount of net plastic strain generated by transformation expansion exceeded the net plastic strain generated by thermal contraction, which entailed tensile residual stress at the surface.

Consequently, appropriately specified quenchant and quenching conditions could guarantee compressive residual stresses at the surface. As indicated by the quenching simulations [12], the tensile residual stress at the surface can be eliminated by quenching conditions which result in a maximum cooling rate shifted towards high temperatures. This type of quenching maximises the magnitude of the compressive residual stress from thermal contraction and minimises the tensile residual stress at the surface from transformation expansion.

The non-uniform residual stress from shot peening, over the spring wire circumference, was caused by the relative orientation of the trajectory of the peening shot and the spring coil (Fig. 9). Shot peening intensity depends on shot impact angle λ . The larger the angle is, the smaller is the transmitted impact energy, the smaller is the compressive residual stress. As indicated by the residual stress distribution curves (Fig. 12), the outermost part of the spring helix (zone 'o' in Fig. 9, $\lambda = 0^\circ$, $\varphi \approx 0^\circ$) receives the largest compressive stress from shot peening, while the top and bottom zones which

are characterised by the largest impact angle λ (zones 't' and 'b' in Fig. 9, $\lambda \approx 90^\circ$, $\varphi \approx \pm 90^\circ$) receive the smallest compressive residual stress. The deviations of the residual stress from compressive to tensile are due to non-uniform shot peening, whose intensity on the top and bottom zones of the spring turns is not sufficient to mask the tensile residual stress after oil-quenching and tempering. The fact that tensile residual stress at the surface was more frequently registered on springs tempered to a higher hardness level (54 HRC) can be rationalised by the diminished stress relaxation during tempering at low temperatures, necessary to attain high hardness levels.

Even if the spring turns were uniformly peened, the magnitude of the compressive residual stress after peening of a surface with tensile residual stress would be smaller compared to a surface with compressive residual stress. This effect is different from the effect of strain peening of leaf springs which are prestrained by elastic bending and the surface with tensile stresses is peened. After the release of the peened spring, larger compressive residual stress is measured compared to a peened spring which had not been prestrained (Xu Jia-chi *et al.* [13]). However during shot peening of spring wire with tensile residual stresses at the surface, there is no possibility for a 'release' and the strain peening effect does not exist. Instead, the compressive component from shot peening superposes with the tensile residual stress component and forms the net residual stress. This is smaller compared to the net residual stress from peening of a surface with compressive residual stress.

Furthermore, the tensile residual stress zones detected on shot peened spring turns, were characterised by a 100% coverage. This means that the compressive stress from shot peening was not sufficient to dominate the tensile residual stress at the surface. Consequently, larger shot peening intensities were necessary to mask the negative effect of the tensile residual stress from oil-quenching and tempering. The intensity of shot peening however, cannot be increased beyond certain level without impairing the fatigue properties. Although shot peening results in work-hardening and beneficial compressive residual stress at the surface, it also damages the surface. While at low tensile stresses from loading, the damage caused by shot peening is compensated by the compressive residual stress, at high loading tensile stresses, the masking effect is nearly lost and many shot-peening craters and folds are identified as fatigue crack origins [6]. The part of the craters and folds causing fatigue failures increased with increasing shot peening intensity.

In order to avoid unfavourable residual stresses at the surface, the latter should be peened at small impact angles. This guarantees a large and uniform compressive residual stress over the spring turns. In order to avoid the tensile residual stresses, another good measure is preventing decarburisation during austenitising. Decarburisation promotes tensile residual stresses at the surface after quenching and diminishes the fatigue strength [14]. It limits the maximum magnitude compressive residual stresses from shot peening, decreases the penetration depth of the compressive residual stress

and increases the surface roughness. Decarburisation also diminishes fatigue resistance of the suspension springs by: (i) diminishing the local fatigue strength due to the decreased density of the surface layer [6, 15], increased grain size and diminished fracture toughness and yield strength; (ii) creating low cycle fatigue conditions for the spring surface.

Acknowledgements

The author thanks Prof. J. F. Knott for the provision of research facilities and the valuable discussions. Gratefully acknowledged is also the financial support from the Department of Trade and Industry and the Science and Engineering Research Council (UK).

References

1. W. E. HEITMANN, T. G. OAKWOOD and G. KRAUSS, in *Fundamentals and Applications of Microalloying Forging Steels*, Proceeding of a Symposium sponsored by the Ferrous Metallurgy Committee of TMS, Edited by Chester J. Van Tyne *et al.* 1996.
2. V. M. SEMENOV and S. M. SEREBRIN, *Soviet Engineering Research* **4**(7) (1984) 28.
3. A. NIKU-LARI, in *First International Conference on Shot Peening*, Paris, 14–17 September (Pergamon Press, Oxford, 1981), p. 1.
4. G. C. BIRD and D. SAYNOR, *Journal of Mechanical Working Technology* **10**(2) (1984) 175.
5. N. K. BURRELL, *SAE Transactions*, Section 3, Vol. 94, paper 850365, 1985.
6. M. T. TODINOV, PhD thesis, The University of Birmingham, School of Metallurgy and Materials, 1999.
7. Rigaku Corporation, "Instruction Manual for Strainflex MSF-2M/PSF-2M," 1994.
8. B. D. CULLITY, "Elements of X-ray Diffraction," 2nd ed. (Addison-Wesley, 1978).
9. SAE J936, Report of Iron and Steel Technical Committee, 1965.
10. K. SHIWAKU, Y. YAMADA, J. KOARAI and Y. KAWAGUCHI, *SAE Transactions*, Section 3, Vol. 94 paper 850364, 1985, p. 3.32.
11. M. T. TODINOV, *Modelling and Simulation in Materials Science and Engineering* **6** (1998) 273.
12. *Idem.*, *ibid.* **7** (1999) 25.
13. XU JIA-CHI, ZHANG DING-QUAN and SHEN BANG-JUN, in *First International Conference on Shot Peening*, Paris, 14–17 September 1981 (Pergamon Press, Oxford) p. 367.
14. M. J. GILDERSLEEVE, *Materials Science and Technology* **7** (1991) 307.
15. YU. M. CHERNYKH, *Metal Science and Heat Treatment* **33**(9/10) (1991) 792.

*Received 20 May
and accepted 16 December 1999*